PHYSICAL REVIEW B **68**, 100501(R) (2003)

Mesoscopic josephson junctions of high-T_c superconductors

A. Ya. Tzalenchuk*
National Physical Laboratory, Queens Road, Teddington, Middlesex TW11 0LW, United Kingdom

T. Lindström, S. A. Charlebois, E. A. Stepantsov,† and Z. Ivanov
Department of Microelectronics and Nanoscience, Chalmers University of Technology and Göteborg University, SE-412 96 Göteborg, Sweden

A. M. Zagoskin‡
D-Wave Systems Inc., 320-1985 Broadway, Vancouver, British Columbia, Canada V6J 4Y3

(Received 14 April 2003; published 5 September 2003)

In this paper we examine the state-of-the-art patterning techniques for fabrication of ultrasmall bicrystal Josephson junctions in $YBa_2Cu_3O_x$. We determine the dependence of junction parameters—critical current, characteristic voltage I_cR_n, and capacitance—on its size. Using the values of the Josephson and the Coulomb energies extracted from experiment, we analyze the dynamics of the junction in zero-bias quantum regime. Finally, we discuss the relevance of parameters, obtained from transport measurements, for the decoherence time in the system.

DOI: 10.1103/PhysRevB.68.100501 PACS number(s): 74.50.+r

I. INTRODUCTION

It is well known that quantum effects gain importance in mesoscopic Josephson junctions.[1] This academic fact was pressed home by recent spectacular demonstrations of macroscopic quantum coherence in Josephson devices (qubit prototypes).

Despite early proposals for qubits based on high-T_c superconductors (HTS's),[2,3] these devices remain in the shadow to a large extent because of the lack of a reliable technology to fabricate structures on the submicrometer scale. Earlier attempts mostly concentrated on making small microbridges without weak links and were largely successful.[4–6] Superconducting microbridges down to 50 nm width were fabricated and characterized.[7] These works demonstrated that in spite of the fragility of the stoichiometry of HTS materials, a high quality epitaxial film can withstand patterning to submicrometer size. When it comes to junctions however, the faster rate of oxygen out-diffusion along grain boundaries and interfaces leads to degradation of superconducting properties as the junction size decreases. Nevertheless, recently, preparation of submicrometer step-edge[8] and ramp[9] Josephson junctions was reported. To the best of our knowledge, the first detailed study of bicrystal Josephson junction of a submicrometer size was presented by Elsner *et al.*[10] Lately, bicrystal grain-boundary Josephson junctions in very thin films were demonstrated.[11]

Dynamics of a small Josephson junction is determined by the interplay of charge and phase degrees of freedom. In the limit, where the phase is a good semiclassical variable, the system can be represented by a fictitious quantum particle with the kinetic energy determined by the capacitance of the junction (Coulomb energy E_C), moving in the potential landscape determined by the phase-dependent critical current (Josephson energy $E_J \gg E_C$). The current-phase relation (CPR) in HTS junctions reflects the complicated symmetry of superconducting wave function and appears to be strongly nonsinusoidal.[12,13] So far the analysis of the influence of this anomalous CPR on the dynamics of mesoscopic junctions was restricted by the lack of experimental data. In this paper we present our version of submicrometer technology for HTS films and investigate ultrasmall bicrystal Josephson junctions in $YBa_2Cu_3O_x$ (YBCO) having in mind their proposed qubit applications.

II. EXPERIMENT

We have fabricated a large number of submicrometer junctions and superconducting quantum interference device on $SrTiO_3$ bicrystals with misorientation angles of 0/32°, 0/40°, and 0/45°. Nominally 250-nm-thick YBCO films were grown by laser ablation using standard parameters. Note that our films are ten times thicker than those studied by Herbstritt *et al.*[11] We believe that relatively thick and short microbridges contain enough oxygen to self-heal the oxygen loss in the grain boundary. In order to protect the film surface and improve adhesion of the post-deposited layers, a 10-nm-thick layer of gold was pulsed laser deposited *in situ* on top of YBCO at room temperature, followed by *ex situ* evaporation of additional 40 nm of gold. Two steps of *e*-beam lithography on polymethyl methacrylate/copolymer double-layer resist were sufficient for fabrication. Resist baking was performed at 135 °C—close to the lower limit for this resist type. Reduced resist baking temperature and the minimum number of processing steps at elevated temperatures minimize oxygen loss. In the first *e*-beam lithography we fabricated gold pads for electrical connections and defined gold alignment marks and rulers for the subsequent processing stages, both 250 nm thick. Since the grain boundary does not give contrast under the electron beam, this pattern was aligned only with respect to the chip corners. Readings were taken from the intersection of the grain boundary with the rulers in an optical microscope, where the grain boundaries are visible due to imperfections and sometimes

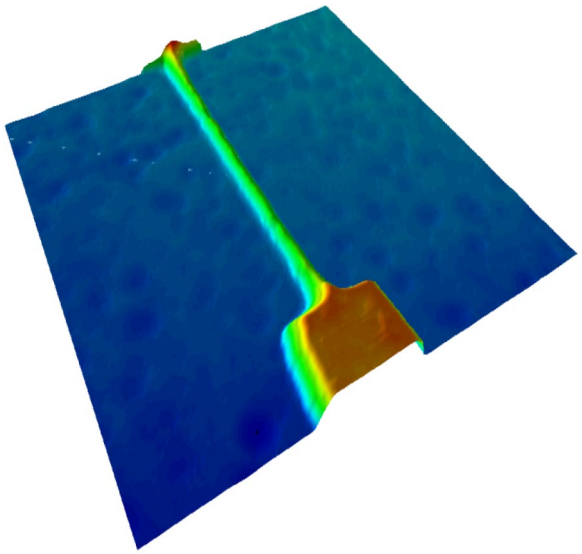

FIG. 1. (Color online) $8\times8\times0.468\ \mu m^3$ atomic force microscope image of a 100-nm-wide bicrystal Josephson junction—the smallest we can make at this time.

due to induced birefringence. The shift and the rotation of the grain boundary with respect to the rulers was then taken into account in the next *e*-beam lithography, which defined the carbon mask for fabrication of the bridges across the bicrystal grain boundary. Alignment could be made with accuracy close to 0.2 μm across the whole substrate. NiCr was used as a masking layer for oxygen plasma etching of carbon. The YBCO was Ar-ion beam etched through the carbon mask during 2 h at 400 eV and 0.1 mA/cm^2. While etching, the substrate was thermally anchored to a 9 °C cold plate to avoid heating and degeneration of the YBCO. Finally, the gold protection layer covering the YBCO was removed by 15-min Ar ion-beam etching at 150 eV and 0.1 mA/cm^2. The result of the completed fabrication process is shown in Fig. 1. It is worth mentioning that even the narrowest of thus prepared junctions are very stable, surviving to-date up to two years without noticeable change in parameters.

III. RESULTS

The dynamical parameters of a mesoscopic Josephson junction can be expressed as a combination of E_J and E_C or explicitly as a function of the critical current I_c and the junction capacitance C. We have measured these parameters at 4.2 K on a large number of Josephson junctions of different dimensions ranging from 0.2 to 4 μm.

In general the critical current of submicrometer junctions did not scale strictly proportionally to the width even though reproducibility in I_c and the normal resistance R_n close to 10% junction to junction on one chip was observed. At the same time the usual scaling of $I_cR_n=j_c\rho_n\propto\sqrt{j_c}$ was confirmed on a large number of submicrometer junctions on different bicrystals (see inset in Fig. 2). Two distinct regions with different slopes can be seen in Fig. 2 with the crossover almost exactly at 1 μm. The crossover might be related to the processing induced damage of the junctions. Interest-

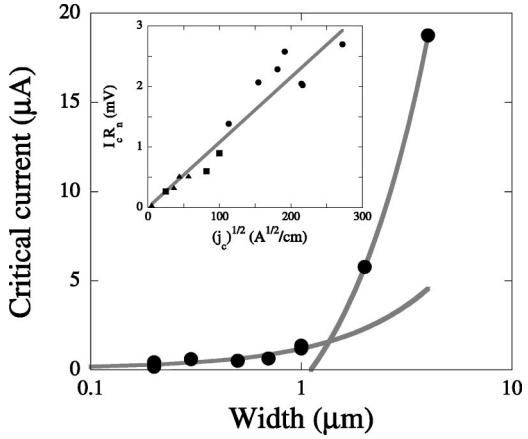

FIG. 2. Critical current as a function of junction width for a 45° grain-boundary junction. The lines are the best linear fits to the data below and above 1 μm; Inset: Scaling of the I_cR_n product with the $\sqrt{j_c}$ measured on two 0/32° and two 0/40° samples.

ingly, however, the large-junction line projects to a finite size of the junction for zero critical current, while the dependence for submicrometer junctions points almost exactly to zero. We therefore speculate that the latter line represents intrinsic properties of the junction barrier, while some other mechanism comes into play on the micrometer scale. For example, this mechanism can be related to high-j_c "shorts" in the barrier.

Most junctions studied in this work were hysteretic by an amount $(I_c-I_r)/I_c\leqslant30\%$ (I_c and I_r are the critical and retrapping currents correspondingly). Applicability of the resistively capacitively shurted junction (RCSJ) model, or equivalently the underlying tilted-washboard potential model, to the dynamics of submicrometer junctions was verified by studying the histograms of the stochastic switching processes between the superconducting and the resistive states of the hysteretic junctions at finite temperatures. The switching currents were determined on successive current sweeps ($\dot{I}\simeq0.1$–10 mA/s) either directly, using a voltage discriminator combined with a sample-and-hold circuit, or from time-of-flight measurements. As can be seen in Fig. 3 (inset) the distributions can be fairly well approximated by the RCSJ expressions. Within this model the junction capacitance can be estimated from the amount of hysteresis following the approximate expression[14] for the Stewart-McCumber parameter

$$\beta_c\equiv(\omega_pR_nC)^2\approx\frac{2-(\pi-2)(I_r/I_c)}{(I_r/I_c)^2},$$

where ω_p is the Josephson plasma frequency. The results for the 40° bicrystal junctions on two different chips are summarized in Fig. 3. As has been previously observed for much wider junctions, the capacitance inversely scales with the junction resistance, yielding $R_nC\simeq1$ ps. In the following section we will provide arguments why this very small time constant does not necessarily spell doom for qubit applications of HTS devices. The values of the junction capacitance are in close agreement with those reported in Ref. 15 for the

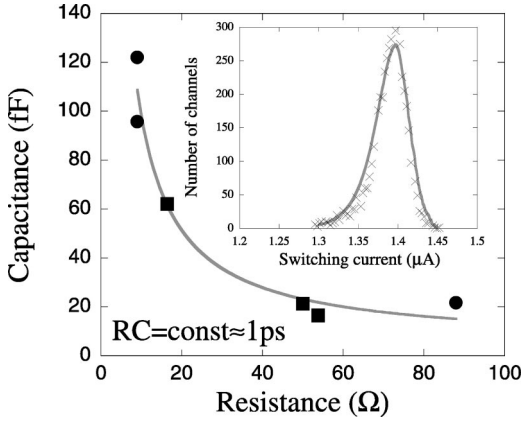

FIG. 3. The junction capacitance as a function of its resistance measured on two 0/40° chips (circles and squares). The best-fit line corresponds to $R_nC \simeq 1$ ps. *Inset*: An experimental switching current distribution histogram and the best fit to the RCSJ model.

junctions of similar resistance. Using the switching histograms, we can estimate the accuracy of parameters determined from single-shot measurements. As can be seen from the figure, the I_c distribution is rather narrow, full width at half maximum equal to (5–7)% of the mean value, which gives the relative error in C determined from the approximation[14] of the order of (30–40)%.

IV. DISCUSSION

Let us first calculate the parameters of submicrometer Josephson junctions, which follow from our experiments. The relation between the Josephson current, energy, and phase difference γ, $I_J(\gamma)=(2e/\hbar)\partial E_J/\partial\gamma$, follows from gauge invariance (and Cooper pair charge being $2e$) and, of course, does not depend on the exact form of $E_J(\gamma)$. Therefore, the nth harmonic of the Josephson energy is related to the nth harmonic of the critical current through $E_{nJ}(\gamma) = \pm\hbar I_n \cos(n\gamma)/2en$. Keeping only the first two harmonics of the current-phase relation, and introducing $\alpha = I_2/I_1$, we reduce the problem to solving the one-dimensional Schrödinger equation for a particle of mass $(\hbar/2e)^2 C$ in thej potential

$$E_J(\gamma) = -E_{1J}\cos(\gamma) + E_{2J}\cos(2\gamma) = -E_{1J}\left[\cos(\gamma) - \frac{\alpha}{2}\cos(2\gamma)\right]. \quad (1)$$

The Hamiltonian of the system is $H = -4E_C\partial_\gamma^2 + E_J(\gamma)$. The ground-state energy of an isolated quantum well is $\hbar\omega_p/2$, where $\hbar\omega_{p1} = 2\sqrt{2E_CE_{1J}}$ for $\alpha \ll 1$, and $\hbar\omega_{p2} = 4\sqrt{2E_CE_{2J}}$ for $\alpha \gg 1$. In order to estimate the tunneling between the minima of E_J, made possible by the "kinetic" Coulomb term, we find the splitting of the energy levels of the two adjacent quantum wells[16] by integrating the momentum $p(E,\gamma)$ between the classical turning points $\pm\gamma_0$ [we neglect the effects of band formation due to periodicity of $E_J(\gamma)$]:

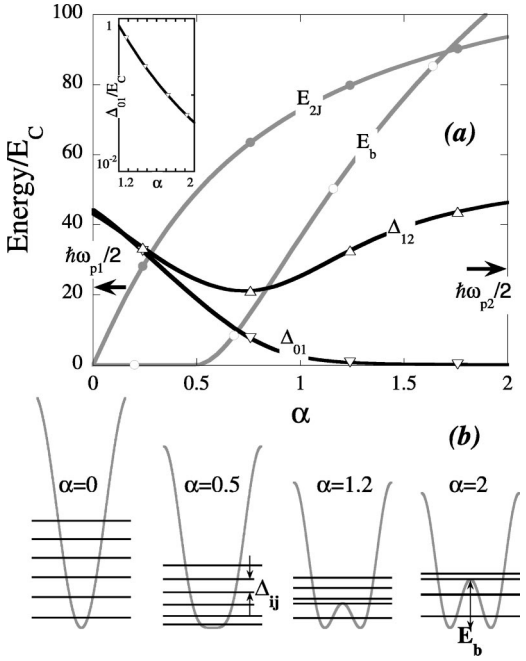

FIG. 4. (a) Level splitting, energy of the second harmonic of the Josephson current, and the barrier height of the double-well potential depending on $\alpha = I_2/I_1$. Arrows indicate the quasiclassical ground-state energies $\hbar\omega_{p1,2}/2$, which are only valid in their respective limits of α. *Inset*: Δ_{01} in more details. (b) Energy level diagrams for several values of α.

$$\Delta \equiv \Delta_{01} = \frac{\hbar\omega_p}{\pi}\exp\left[-\frac{1}{\hbar}\int_{-\gamma_0}^{\gamma_0}\left|p(\hbar\omega_p/2,\gamma)\right|d\gamma\right] = \frac{\hbar\omega_p}{\pi}\exp\left[-\frac{1}{2}\int_{-\gamma_0}^{\gamma_0}d\gamma\sqrt{\frac{E_J(\gamma)-\hbar\omega_p/2}{E_C}}\right]. \quad (2)$$

For example, if the second harmonic dominates, we obtain

$$\Delta = \frac{\hbar\omega_p}{\pi}\exp\left(-\left[\frac{2E_{2J}}{E_C}\right]^{1/2}F\left(\sqrt{2E_C/E_{2J}}\right)\right), \quad (3)$$

where $F(z) = \sqrt{1-z}E[\arccos\sqrt{z}|(1-z)^{-1}]$, and $E(a|b)$ is the elliptic integral of second kind.

In reality $\alpha \approx 1$, and we have to calculate the eigenstates numerically. For a given α, the amplitude of the first harmonic of the Josephson current can be obtained from the measured critical current $I_c \approx 1\ \mu$A, using $I_c = I_1 \max_\gamma\{\sin(\gamma) - \alpha\sin(2\gamma)\}$. The capacitance of the junction was taken to be 10^{-14} F (Fig. 3), corresponding to $E_C/k_B \approx 93$ mK. The results of numerical calculations of different energies as a function of α for this choice of I_c and C are presented in Fig. 4. Above $\alpha = 0.5$ the potential becomes bistable, and as the barrier height E_b increases, so does the spacing between the ground state (split by tunneling) and the higher excited levels. This makes the junction a quasi-two-level system, since the transitions to the higher levels are suppressed. Indeed, for α in the range 1.2–1.7 the splitting between the first and second eigenvalues (100 mK) is one to two orders of magnitude less than the energy difference with the next eigenvalue (>3 K). They can therefore be consid-

ered well decoupled for sub-Kelvin operating temperatures. As an example, for $\alpha=1.2$, $I_c=1$ μA and $C=10^{-14}$ F we obtain the following: $E_C=e^2/2C$ corresponds to 2 GHz or 100 mK; $I_1=0.5$ μA; $I_2=0.6$ μA; $E_{1J}/E_C=131$; $E_{2J}/E_C=79$; $\hbar\omega_p=15$–$25E_C$ (30–50 GHz); $\Delta_{01}/E_C=0.8$ (1.6 GHz or 80 mK), and $\Delta_{12}/E_C=32$ (64 GHz or 3.2 K).

The question of decoherence rate in HTS junctions is still not resolved, though the possibility to observe coherent quantum behavior in these systems hinges on the answer to it. As we noted above, the transport measurements provide the R_nC constant of the order of 1 ps, seemingly closing the door on any possibility to use the HTS materials as quantum bits. Nevertheless such a conclusion could be too hasty. Recently, the decoherence in d/d junctions was considered theoretically.[17] These results question the relevance of R_nC as a measure of damping at zero bias. Indeed, R_n is obtained in the resistive regime, when the phase runs along the washboard potential, and dissipative quasiparticle current is always present. On the contrary, in the ''qubit'' regime the external bias is absent, and the phase is localized. The quasiparticle current only arises due to tunneling between the minima of the potential, which produces ac Josephson voltage: $I(V=\hbar\omega/e=\Delta_{01}/e)$. The main contributions to this low-bias quasiparticle current will be given by midgap Andreev bound states (MGS's) and nodal quasiparticles. The significance of each of these factors depends on the mismatch angle, type of the grain boundary (symmetric or asymmetric), roughness of the interface, and its transparency. As shown by Fominov and Golubov, the most dangerous contribution is due to MGS-to-MGS scattering leading to a zero-bias conductance peak. However, MGS's can be split by several mechanisms, which shifts this peak to higher biases and therefore suppresses this decay channel (for a discussion of phenomena related to Andreev bound states, see the detailed review[18] and references therein). The nodal quasiparticles contribute much less close to zero bias, since this term scales as ω^2. Experimental I-V characteristics of 0/45° grain-boundary junctions (where MGS's are formed only on one side of the interface and therefore only MGS-to-node contribution is significant) show significantly suppressed admittance close to zero bias compared to R_n.

To summarize this discussion, the value of quasiparticle resistance R_n, determined from transport measurements and used above as the natural scaling parameter for the capacitance, is likely irrelevant to decoherence in d/d junctions. On the contrary, the energies E_J and E_C, derived from the same measurements, are correct.

ACKNOWLEDGMENTS

We are indebted to A. Golubov and Ya. Fominov for communicating their results prior to publication and many helpful comments. Discussions with M. H. S. Amin, T. Claeson, J. C. Gallop, A. Maassen van den Brink, and A. Yu. Smirnov are gratefully acknowledged.

*Email address: alexander.tzalenchuk@npl.co.uk

†On leave from Institute of Crystallography, Russian Academy of Sciences, 59 Leninski pr., 117 333 Moscow, Russia.

‡Also at Physics and Astronomy Dept., The University of British Columbia, 6224 Agricultural Rd., Vancouver, Canada V6T 1Z1.

[1] M. Tinkham, *Introduction to Superconductivity*, 2nd ed. (McGraw-Hill, New York, 1996), Chap. 7.

[2] L. Ioffe, V. Geshkenbein, M. Feigel'man, A. Fauchre, and G. Blatter, Nature (London) **398**, 679 (1999).

[3] A. Blais and A. Zagoskin, Phys. Rev. A **61**, 042308 (2000).

[4] R. Barth, B. Spangenberg, C. Jaekel, H. Roskos, H. Kurz, and B. Holzapfel, Appl. Phys. Lett. **63**, 1149 (1993).

[5] J. Schneider, H. Kohlstedt, and R. Wordenweber, Appl. Phys. Lett. **63**, 2426 (1993).

[6] H. Assink, A. Harg, C. Schep, N. Chen, D. Marel, P. Hadley, E. Drift, and J. Mooij, IEEE Trans. Appl. Supercond. **3**, 2983 (1992).

[7] P. Larsson, B. Nilsson, and Z. Ivanov, J. Vac. Sci. Technol. B **18**, 25 (2000).

[8] P. Larsson, A. Tzalenchuk, and Z. Ivanov, J. Appl. Phys. **90**, 3450 (2001).

[9] P. Komissinski, B. Hogberg, A. Tzalenchuk, and Z. Ivanov, Appl. Phys. Lett. **80**, 1022 (2002).

[10] H. Elsner, R. Ijsselsteijn, W. Morgenroth, H. Roth, and H.-G. Meyer, Microelectron. Eng. **41-42**, 407 (1998).

[11] F. Herbstritt, T. Kemen, L. Alff, A. Marx, and R. Gross, Appl. Phys. Lett. **78**, 955 (2001).

[12] E. Il'ichev *et al.*, Phys. Rev. Lett. **86**, 5369 (2001).

[13] T. Lindström, S. Charlebois, A. Tzalenchuk, Z. Ivanov, M. Amin, and A. Zagoskin, Phys. Rev. Lett. **90**, 117002 (2003).

[14] H. Zappe, J. Appl. Phys. **44**, 1371 (1973).

[15] P. McBrien, R. Hadfield, W. Booij, A. Moya, M. Blamire, E. Tarte, J. Clark, and C. Pegrum, IEEE Trans. Appl. Supercond. **9**, 3468 (1999).

[16] L. Landau and E. Lifshitz, *Quantum Mechanics: Non-relativistic Theory*, 3rd ed. (Pergamon Press, Oxford, 1977), Vol. 3, Chap. 7, sec. 50.

[17] A. Golubov and Y. Fominov (unpublished); M.H.S. Amin (private communication); A.N. Omelyanchouk, Yu. Kolesnichenko, and A.M. Zagoskin (private communication).

[18] T. Löfwander, V. Shumeiko, and G. Wendin, Supercond. Sci. Technol. **14**, R53 (2001).